A high-resolution downscaled CMIP5 projections dataset of essential surface climate variables over the globe coherent with the ERA5 reanalysis for climate change impact assessments

Thomas Noël, Harilaos Loukos, Dimitri Defrance, Mathieu Vrac, Guillaume Levavasseur

Data in Brief 35 (2021) 106900

Contents lists available at ScienceDirect

Data in Brief

journal homepage: www.elsevier.com/locate/dib

Data Article

A high-resolution downscaled CMIP5 projections dataset of essential surface climate variables over the globe coherent with the ERA5 reanalysis for climate change impact assessments

Thomas Noël[a,*], Harilaos Loukos[a], Dimitri Defrance[a], Mathieu Vrac[b], Guillaume Levavasseur[c]

[a] *The Climate Data Factory*[1], *Paris, France*
[b] *Laboratoire des Sciences du Climat et de l'Environnement (LSCE-IPSL), CEA/CNRS/UVSQ, Université Paris-Saclay Centre d'Etudes de Saclay, Orme des Merisiers, 91191 Gif-sur-Yvette, France*
[c] *Institut Pierre Simon Laplace, SU/CNRS, Paris, France*

ARTICLE INFO

Article history:
Received 4 December 2020
Revised 16 February 2021
Accepted 17 February 2021
Available online 21 February 2021

Keywords:
High-resolution
Projections
CMIP5
ERA5
Downscaling
Climate change
Adaptation
Impact modeling

ABSTRACT

A high-resolution climate projections dataset is obtained by statistically downscaling climate projections from the CMIP5 experiment using the ERA5 reanalysis from the Copernicus Climate Change Service. This global dataset has a spatial resolution of 0.25°x 0.25°, comprises 21 climate models and includes 5 surface daily variables at monthly resolution: air temperature (mean, minimum, and maximum), precipitation, and mean near-surface wind speed. Two greenhouse gas emissions scenarios are available: one with mitigation policy (RCP4.5) and one without mitigation (RCP8.5). The downscaling method is a Quantile Mapping method (QM) called the Cumulative Distribution Function transform (CDF-t) method that was first used for wind values and is now referenced in dozens of peer-reviewed publications. The data processing includes quality control of metadata according to the climate

* Corresponding author.
E-mail address: thomas@theclimatedatafactory.com (T. Noël).
Social media: (T. Noël), (H. Loukos), (D. Defrance)
[1] @TheClimDatFac

https://doi.org/10.1016/j.dib.2021.106900

modeling community standards and value checking for outlier detection.

Specifications Table

Subject	Climatology; Global and Planetary Change
Specific subject area	Climate change; Natural disasters. Evolution of temperature, precipitation and others climate variables
Type of data	Data Cube (Raster X Time) in NetCDF
How data were acquired	CMIP5 model projections data were obtained from the Copernicus Climate Change Service and Earth System Grid Federation data nodes. A statistical downscaling trend-preserving method (CDFt) was applied using the ERA5 reanalysis for calibration.
Data format	Netcdf: is a set of software libraries and self-describing, machine-independent data formats that support the creation, access, and sharing of array-oriented scientific data (use in Atmospheric and Oceanic sciences).
Parameters for data collection	Statistical downscaling with the CDFt method and ERA5 reanalysis historical data: 0.25° × 0.25° spatial resolution, calibration period 1981–2010, historical and future period from 1950 to 2100 for 21 models and 2 scenarios (RCP4.5 and RCP8.5), monthly temporal resolution, raster data.
Description of data collection	Simulated near-surface air Temperature (mean, minimum, maximum), precipitation, and mean near-surface wind speed data from 21 climate models downloaded at the Earth System Model Grid Federation (https://esgf-node.ipsl.upmc.fr/search/cmip5-ipsl/) and Copernicus Climate Change Service (https://cds.climate.copernicus.eu) including the ERA5 reanalysis data for the period 1981–2010 and the same variables.
Data source location	Global scale, including land ocean surface
Data accessibility	Accessible through Earth System Grid Federation (ESGF) under research only license at https://esgf-node.ipsl.upmc.fr/projects/c3s-cmip5-adjust/
Related research article	Michelangeli, P. A., Vrac, M., & Loukos, H. (2009). Probabilistic downscaling approaches: Application to wind cumulative distribution functions. Geophysical Research Letters, 36(11), GL038401. Vrac, M., Noël, T., & Vautard, R. (2016). Bias correction of precipitation through Singularity Stochastic Removal: Because occurrences matter. Journal of Geophysical Research: Atmospheres, 121(10), 5237–5258.

Value of the Data

- The high resolution, number of models and variables available offer a great opportunity for both researchers and climate change adaptation practitioners to study climate change features and feed this data into impact models for any region around the world.
- The dataset is obtained by statistically downscaling climate projections from the CMIP5 experiment using the ERA5 reanalysis from the Copernicus Climate Change service, a data product extensively used around the world for historical climate analysis. A great advantage of this dataset is thus to provide an extension of the ERA5 reanalysis into the future.
- The dataset is global, has a spatial resolution of 0.25°x 0.25°, comprises 21 climate models allowing to address model uncertainty and includes 5 surface daily variables at monthly resolution: air temperature (mean, minimum, and maximum), precipitation, and mean near-surface wind speed.
- To sample future climate uncertainty from anthropogenic forcing, two greenhouse gas emissions scenarios are available: one with mitigation policy (RCP4.5) and one without mitigation (RCP8.5).

1. Data Description

The high-resolution climate projections dataset covers the globe at a 0.25°x0.25° spatial resolution and at monthly temporal resolution for five surface variables. It comprises 21 models (see Table 1) from the CMIP5 experiment [1] with simulations for the historical period (1950–2005) and the 21st century (2006 to 2100) under two emissions scenarios: one with mitigation policy (Representative Concentration Pathway 4.5 or RCP4.5) and one with no mitigation (Representative concentration Pathway 8.5 or RCP8.5). The following five surface land and ocean variables are downscaled: mean daily temperature, daily minimum and maximum temperature (at 2 m), total precipitation, and surface wind speed (at 10 m). The combination of models and scenarios represents 36 climate projections including all variables except for a few models that didn't provide some (see Table 1). Other variables, models and emissions scenarios could be added in the near future.

The data was produced with a statistical downscaling method using the ERA5 reanalysis [2] for calibration and training (see next section for details). The interest of the downscaled data is the removal of model biases at a resolution more compatible with the requirements of assessments and further modeling of the impacts of climate change. In other terms it corrects the climatology (distribution) of model values to make them comparable with a reference observational dataset [3], which in this case is the ERA5 reanalysis. In the following subsections, we present the file naming conventions then proceed an illustration of the bias removal over the historical period and the climate change signal differences at the end of century.

1.1. File name conventions

There is no official Data Reference Syntax (DRS) defined by the climate modeling community for statistically bias-adjusted or downscaled CMIP projections as there is for CMIP5 projections. However, there is a DRS for CORDEX bias adjusted simulations defined in the context of the EURO–CORDEX experiment. We adapted the EURO–CORDEX DRS for adjusted projections to CMIP5 in order to produce a DRS for CMIP5 adjusted projections [4].

Table 1
The CMIP5 models list with the availability of the essential surface variables: temperature (minimum –tasmin-, maximum –tasmax-, and daily mean –tas-), precipitation –pr- and wind speed -sfcWind-).

GCM	Historical	RCP4.5	RCP8.5
inmcm4 (INM, Russia)	No sfcWind	No sfcWind	No sfcWind
ACCESS1–0 (BoM-CSIRO, Australia)	All	All	All
ACCESS1–3 (BoM-CSIRO, Australia)	All	All	All
bcc-csm1–1 (BCC, China)	No sfcwind	No sfcWind	No pr, sfcWind
bcc-csm1–1-m (BCC, China)	No sfcWind	No sfcWind	No sfcWind
BNU-ESM (BNU, China)	All	All	All
CMCC–CM (CMCC, Italy)	No sfcWind	No sfcWind	No pr and sfcWind
CMCC–CMS (CMCC. Italy)	All	None	All
CNRM-CM5 (CNRM-CERFACS, France)	All	All	None
GFDL-CM3 (NOAA, USA)	All	All	All
GFDL-ESM2G (NOAA, USA)	All	All	All
GFDL-ESM2M (NOAA, USA)	All	All	All
HadGEM2-CC (UK Met Office, UK)	All	All	All
HadGEM2-ES (UK Met Office, UK)	All	All	All
IPSL-CM5A-LR (IPSL, France)	All	All	All
IPSL-CM5A-MR (IPSL, France)	All	All	All
IPSL-CM5B-LR (IPSL, France)	All	All	All
MIROC5 (UTCCSR, Japan)	All	All	All
MPI-ESM-LR (MPI, Germany)	All	All	All
MPI-ESM-MR (MPI, Germany)	All	All	All
NorESM1-M (NCC, Norway)	No sfcWind	No sfcwind	No sfcWind

We kept the term “bias-adjustment” and “adjustment” even if strictly speaking we are producing downscaled projections. The terms “bias-adjusted” and “downscaled” are used interchangeably in the scientific literature because they often involve the same statistical techniques (even though, more recently, bias-adjustment is reserved for cases where the original model resolution is unchanged). We also wanted to use only what was defined by the climate modeling community. On top of this, it appears to us the DRS is sufficient to include all the information needed in the file naming.

The DRS we came up for CMIP5 adjusted projections is presented below through a short illustrative example of file naming:

- data file containing original (uncorrected) model results:
  tas_day_IPSL-CM5A-MR_rcp45_r1i1p1_20060101–20151231.nc
  where:
  - “tas” is the conventional name for surface temperature,
  - “day” is the label for frequency (here daily)
  - “IPSL-CM5A-MR” is the official name of the climate model,
  - “rcp45” is the short name of the used Representative Concentration Pathway,
  - “r1lip1” is the member number of the simulation,
  - “20060101–20151231″ are the start and end date of the simulation.

- bias-adjusted data file (new/modified information in bold)
  tas**Adjust**_Amon_IPSL-CM5A-MR_rcp45_r1i1p1_**gr025_TCDF-CDFT23-ERA5–1981–2010**_200601–201512.nc
  where:
  - “Adjust” is added to the variable conventional name,
  - “Amon” is the label for frequency (here monthly),
  - “gr025” is the grid label of the downscaled data,
  - “TCDF” is the short name of the organization that performed the post-processing,
  - “CDFT23” is the label referencing the method,
  - “ERA5” the short name of the data set used as observations,
  - “1981–2010″ is the period used for statistical calibrating the method.

The complete list of the data files is given in Annex 1.

1.2. Differences between interpolated and downscaled data with reanalysis data

Here we compare the differences with the ERA5 reanalysis of both the original model (interpolated on the reanalysis grid and referred to as “interpolated”) and downscaled simulations (referred to as “downscaled”). We first look at the historical 30-year calibration period (1981–2010) for daily mean temperature, total precipitation and wind speed. We also look at the 1951–1980 period but for simulations only (since there is no reanalysis data) to see the differences in a 30-year period different from the calibration period.

In Fig. 1, we illustrate the spatial differences between the interpolated (left) and downscaled data (right) over the calibration period. For temperature, the ensemble mean of CMIP5 models tends to overestimate temperature. This is particularly true for northern America where the bias between the model mean and ERA5 is above $+5\,^{\circ}C$. We can further notice that temperature in mountainous areas (Himalaya and the Rockies) is often underestimated by GCMs because of the poor representation of elevation. When considering the downscaled data, models have a temperature comparable to the ERA5 reanalysis over the world. For precipitation, there are overestimations of precipitation over the oceans in the tropics, along the Andes Cordillera, south of the Arabian Peninsula or in the Gulf of Guinea. On the contrary, there is an underestimation of rainfall in the areas adjacent to the previous ones (e.g. West Africa). For wind speed, we have an

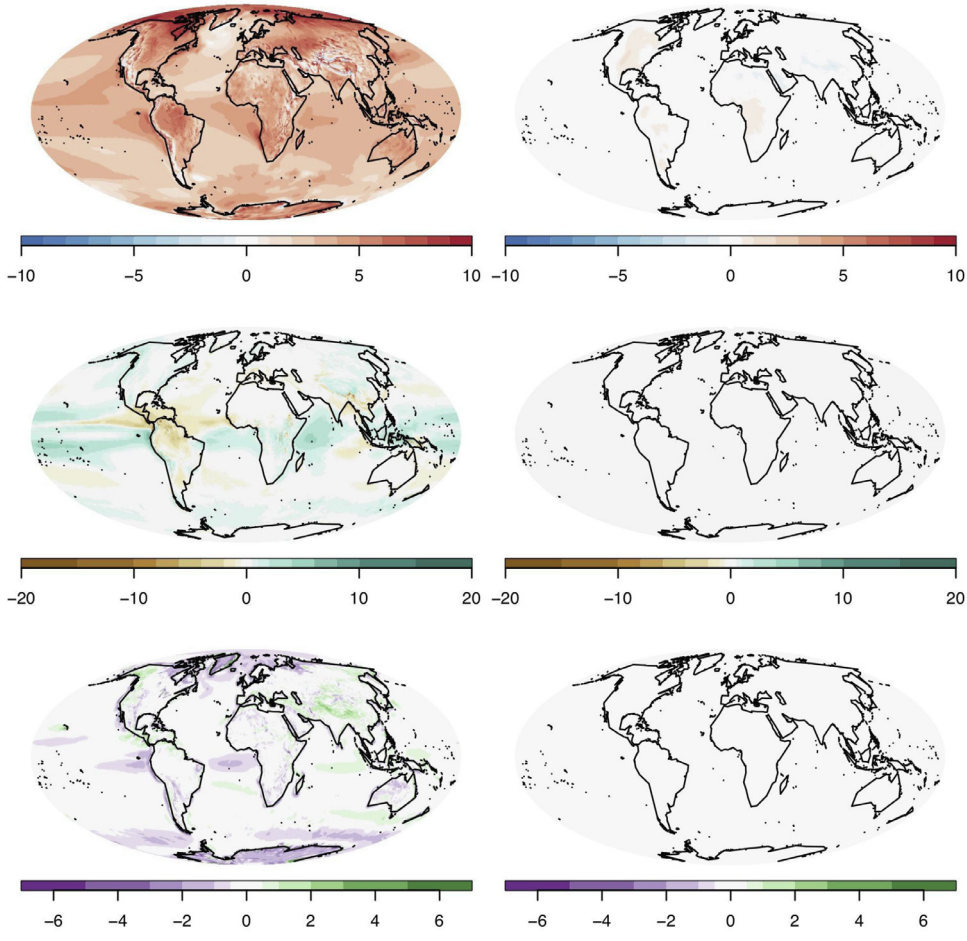

Fig 1. Comparison between the interpolated data and the downscaled data averaged over the calibration period (1981–2010), for temperature (°C) (top), for precipitation (mm/day) (center) and for wind speed (m/s) (below). Difference between the interpolated and reanalysis data (left) and the downscaled and reanalysis data (right).

underestimation in the North (Greenland) and in Antarctica. In the mountainous area (Himalaya, The Rockies), we have an underestimation for interpolated data. The underestimation is closed with the downscaled data.

In Fig. 2a, the cumulative distributions functions (CDFs) are empirically estimated from monthly values averaged on the globe for the interpolated (left) and for downscaled data (right) over the calibration period. There is a spread between the ERA5 reanalysis and the interpolated data with overestimations and underestimations. This spread is more important for precipitation and wind speed than for the temperature. For downscaled data, the difference between the simulations CDFs and observation CDFs is very diminished. However, for precipitation, we observe differences for low and high monthly precipitation amounts. This is due to the fact that downscaling is performed at a daily scale and grid point by grid point, while CDFs are estimated on monthly and spatially-averaged data. The day-to-day (temporal) and spatial variability of the model data are preserved by the downscaling method, however residual biases can appear on monthly and spatial averages.

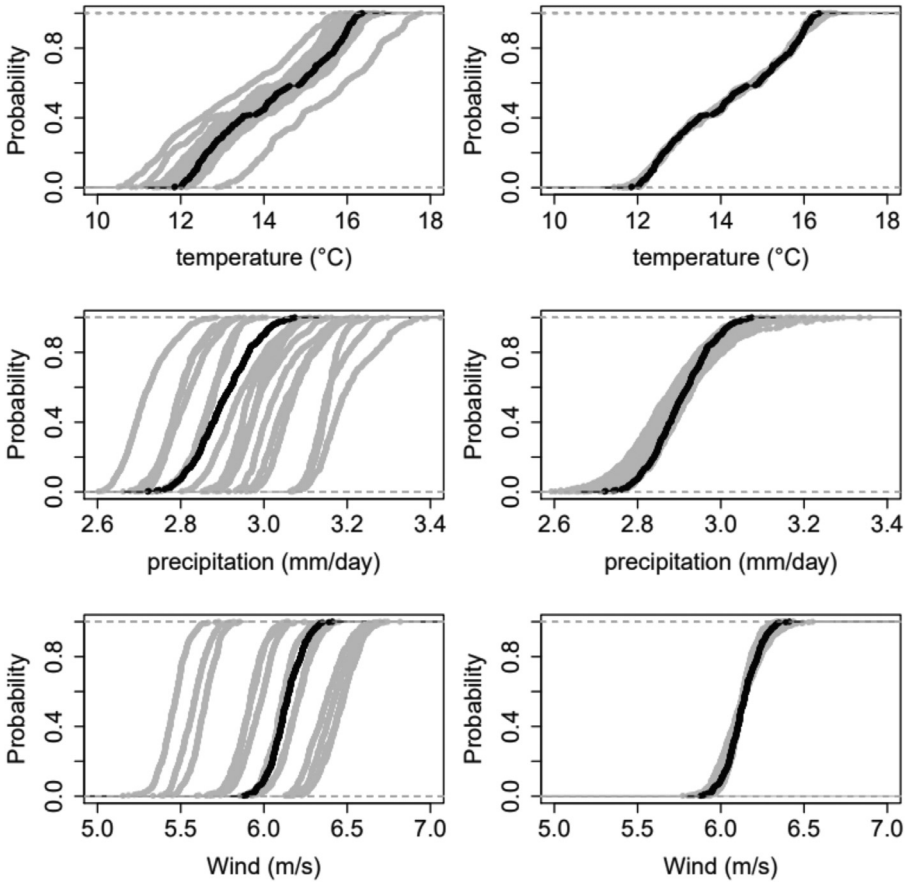

Fig 2a. Cumulative distribution functions of global domain mean monthly averages over the calibration period (1981–2010), for temperature (top), for precipitation (center) and for wind speed (below). In gray the results for each model for interpolated data (left) and for downscaled data (right) and in black the ERA5 reanalysis.

Fig. 2b, is the same as Fig. 2a but over the 1951–1980 period. We can see the same type of changes between the interpolated and downscaled data and of features among the variables as over the calibration period. In the interpolated data, the spread of cumulative distributions is similarly more important for precipitation and wind speed than for temperature. The reduction of CDFs spread in the downscaled data is more pronounced for temperature and wind speed than precipitation.

1.3. Changes at the end of the century after downscaling

Here we illustrate changes by the end of the century over the 2071–2100 period under scenario RCP8.5, comparing the interpolated and downscaled simulations. The analyses are based on daily mean temperature, total precipitation and surface wind speed.

On the maps of Fig. 3, we show the spatial difference between interpolated and downscaled data of the ensemble mean. For temperature, the effect of downscaling is observed mainly in mountainous regions as in the Himalayan massif, the Andes and in the Rockies. For precipitation, we can see severe underestimation in the tropics and particularly in South America, West Africa,

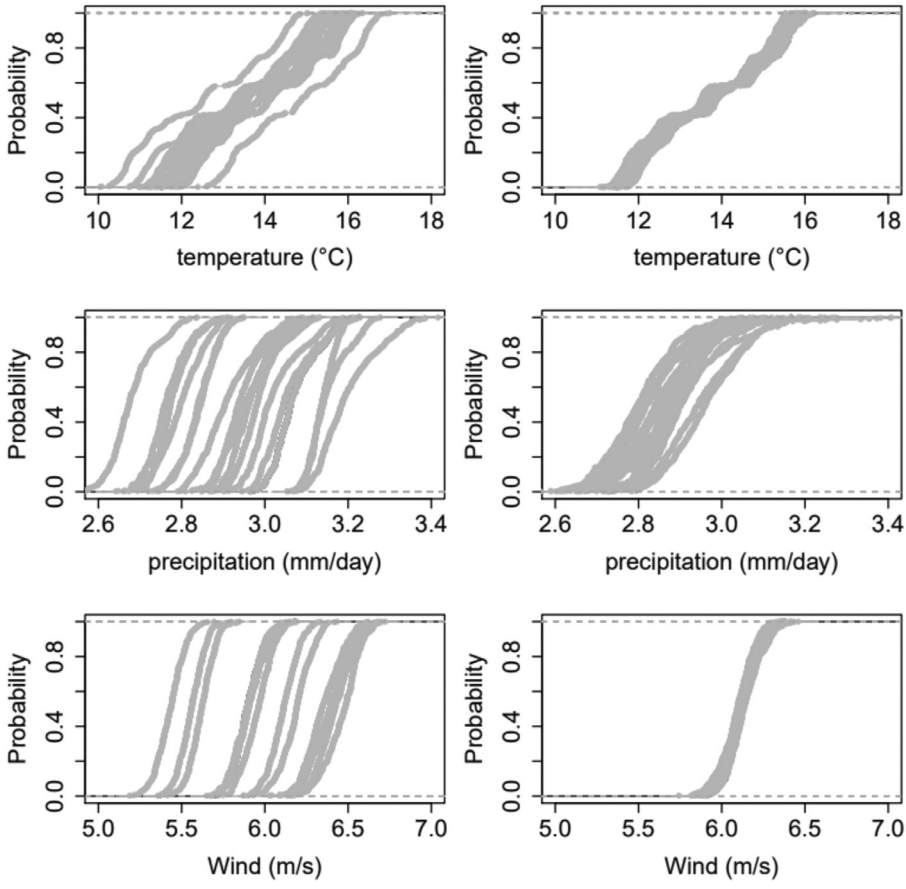

Fig 2b. Cumulative distribution functions of global domain mean monthly averages over the validation period (1951–1980), for temperature (top), for precipitation (center) and for wind speed (below). In gray the results for each model for interpolated data (left) and for downscaled data (right).

India and Oceania. We can also notice that the simulated double ITCZ in the Pacific (e.g. [5]) is corrected. In extra-tropical areas, the corrections are smaller between -2 and $+2$ mm/day. For wind speed, as in Fig. 1, the poles show stronger wind speed in the downscaled data and lower wind speed for the mountainous regions.

In Fig. 4, we now illustrate the difference between interpolated and downscaled data in terms of time series of annual averages. For all variables, while maintaining the general trend linked to the climate scenario, there is a reduction of the ensemble envelope due to the reduced inter-model differences that is quantified by the distribution shown on the boxplots. For temperature, the strong warming trend is maintained with an alignment of the ensemble median at the center of the envelope. For precipitation, the general trend linked to the climate scenario is now stronger and the interannual variability more visible. For wind speed, there is no clear trend and evolution seems similar to the historical period. The ensemble envelope is smaller than for observations partly due to the spatial and temporal averaging smoothing, a feature less pronounced at smaller scales (e.g. monthly point data).

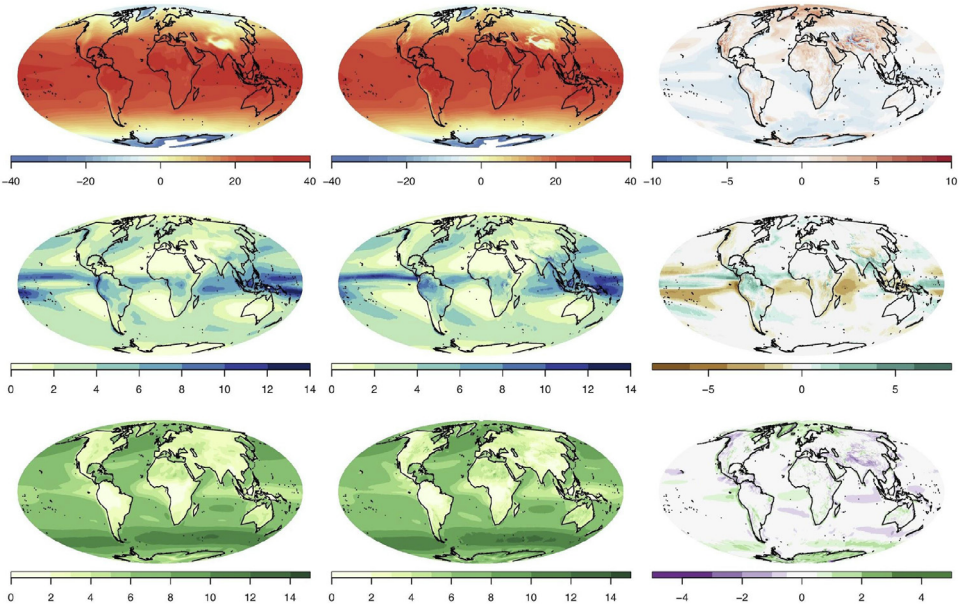

Fig 3. Changes of the ensemble mean averaged over the end of the century (2071–2100), for temperature (°C) (top), precipitation (mm/day) (center) and wind speed (m/s) (below). Interpolated data (left), downscaled data (center), and difference between downscaled and interpolated data (right).

2. Experimental Design, Materials and Methods

Four datasets are used in this work:

- The reanalysis data that is used as reference for calibrating the statistical algorithm over a training period. The reanalysis grid sets the final resolution of the downscaled projections.
- The original model climate projections that come in a variety of spatial resolutions (typically between 2.0°x2.0° and 0.75°x0.75°) and referred to as “raw”.
- The raw data interpolated on the reanalysis grid and referred to as “interpolated”.
- The downscaled data obtained from the interpolated data and the reanalysis data used for statistical calibration (both on the same grid) and referred as “downscaled”.

The raw and reanalysis data are input data that need to be sourced. The interpolated data is just an intermediary dataset needed by the methodology while the downscaled data is the final dataset. These datasets correspond to the four steps process (data sourcing, remapping, downscaling, quality control) described below.

2.1. Data sourcing

The reanalysis data is the ERA5 reanalysis [2]. ERA5 is the latest climate reanalysis being produced by ECMWF as part of implementing the EU- funded Copernicus Climate Change Service (C3S), providing hourly data on atmospheric, land-surface and sea-state parameters together with estimates of uncertainty from 1979 to present day. ERA5 data are available on the C3S Climate Data Store on regular latitude-longitude grids at 0.25° x 0.25° resolution. We compute the daily data from the ERA5 hourly data for all necessary variables.

The climate simulations hail from The Coupled Model Intercomparison Project Phase 5 (CMIP5) experiment [1]. They support the Fifth Assessment Report (AR5) of the Intergovern-

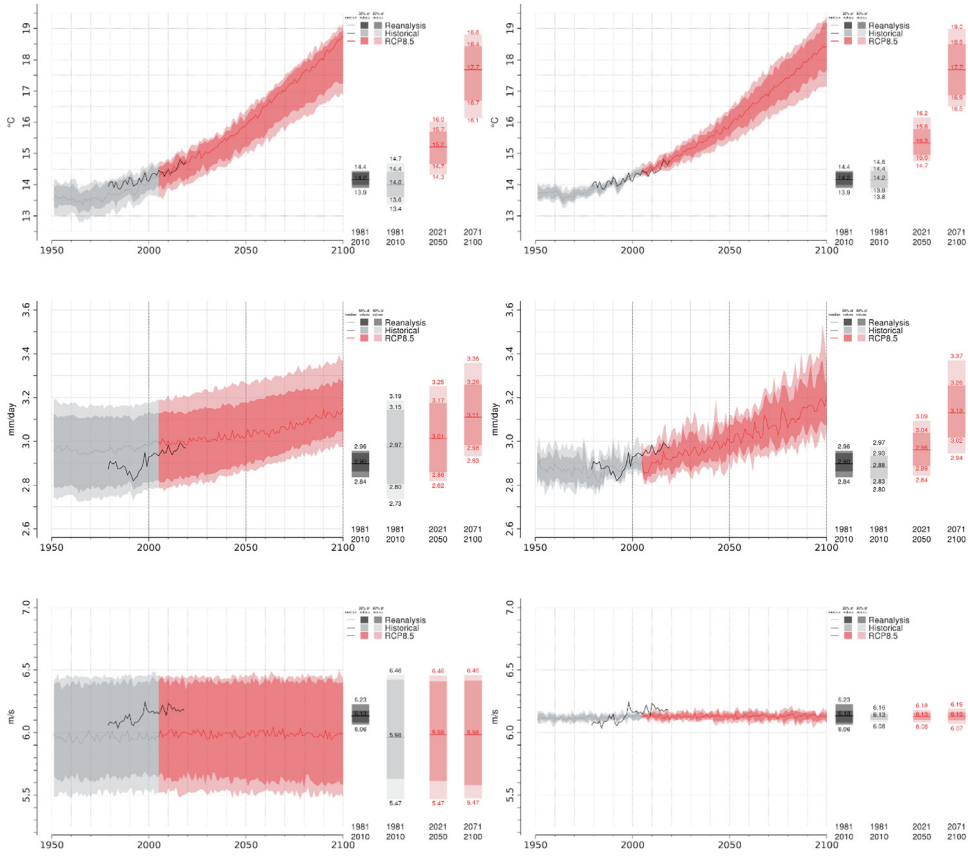

Fig 4. Time series of spatially averaged annual mean model results (1950–2100) and ERA5 reanalysis (1979–2020), for temperature (top), precipitation (center), and wind speed (below). The interpolated data (left) and the downscaled data (right). Envelope of model results are in shades of gray over the historical period (1950–2005) and in shade of red over the projection period (2006–2100). Median of model results is in plain line and ERA5 reanalysis data is plotted for comparison as a plain black line. Boxplots representing the distribution of values are also plotted.

.

mental Panel on Climate Change (IPCC). We use projections from 2 emissions scenarios: RCP4.5 (moderate mitigation policy scenario) and RCP8.5 (a no mitigation policy scenario). Daily data of necessary variables are extracted from the Copernicus Climate Change Service that hosts a subset of the CMIP5 archive. The data covers the period from January 1st 1950 to December 31st 2100 (except for some models). All models have different spatial resolutions ranging between 0.75° to 3° The list of models is shown on Table 1.

2.2. Remapping

Remapping is a preliminary task required by the downscaling methodology. It consists in spatially interpolating the raw simulations (between 0.75° and 3° resolution) onto the ERA5 grid (0.25° x 0.25°). We use the Climate Data Operators (CDO, 2016) software from the Max Planck Institute that gathers various algorithms for interpolation used by the scientific community. Daily temperature (mean, minimum, maximum) and daily wind speed are interpolated with

a bicubic method. Daily precipitation is interpolated sequentially (to 1.5° then to 0.75°, and then 0.25°) with a conservative method.

2.3. Downscaling

The downscaling method applied here is a Quantile mapping-based method (QM) called the Cumulative Distribution Function transform (CDF-t) method [6–10]. CDF-t was first developed for wind values and is now referenced in dozens of peer-reviewed publications to downscale different sets of data and variables (e.g. [11–13]). QM methods relate the cumulative distribution function of a climate variable at large scale (e.g., from the GCM) to the CDF of the same variable at a local scale (e.g., from the reanalysis). They are increasingly popular in climate applications although bias correction methods have received criticism (e.g. [14]). For a review of recent QM methods see [3]. In our case the variables are downscaled at a daily resolution over the 1951–2100 period using 1981–2010 as calibration period. The precipitation variable is downscaled with a specific version of CDF-t referred to as "Singularity Stochastic Removal" (SSR) which considers rainfall occurrence and intensity challenges [15]. The last step is to average daily values into monthly ones to construct the dataset.

2.4. Standardization

Standardization consists in rewriting output data files and related metadata to comply with standards used by the climate modeling community (e.g., the Climate and Forecast metadata convention and the Data Reference Syntax). We use the Climate Model Output Rewriter 2 (CMOR 2) library.

2.5. Quality control

We conduct two types of quality control. The first one is technical and consists in verifying data compliance with climate community's standards, data consistency and metadata. Doing quality control is crucial for the data publication process and data re-use. The second quality control is a value check to check for outlier values in the downscaled data.

2.5.1. Technical quality control

We use the Quality Assurance tool (QA-DKRZ, https://readthedocs.org/projects/qa-dkrz) developed by the Deutsches Klimarechenzentrum (DKRZ) to check conformance of meta-data of climate simulations given in NetCDF format with conventions and rules of projects. During the Quality Assurance process of the DKRZ, the following criteria are checked:

1 Number of datasets is correct and > 0
2 Size of every dataset is > 0
3 The datasets and corresponding metadata are accessible
4 The data sizes are controlled and correct
5 The spatial-temporal coverage description "metadata" is consistent with the data,
6 Time steps are correct and the time coordinate is continuous
7 The format is correct
8 Variable description and data are consistent

2.5.2. Value quality control

The value quality control is built with CDO and NCO tools and consists in:

- Analyzing the difference between the downscaled values and the observations over the reference period.
- Analyzing the time evolution difference between downscaled and original model.

2.5.3. Difference between downscaled model and observations

First, we estimate two quantities:

- The average for each month over the reference period of the observations.
- The average for each month over the reference period of the downscaled model.

We then estimate the difference between these two quantities for every month. For each month we take the 10th and 90th quantiles. That gives 12 values for each quantile.

Finally, we verify that these 12 values are comprised in the following ranges (unpublished, R. Vautard personal communication):

- temperature between [−1; 1] in K,
- precipitation between [−0.5; 0.5] in mm.day-1,
- surface wind speed between [−0.5; 0.5] in m.s-1.

These values are relatively small and allow only low discrepancies since modifications should be small over the historical period (inherently over the calibration period). If values are outside the range, the script raises an error and the simulation is rejected and thus not included in the dataset.

2.5.4. Difference of evolutions between downscaled model and original model

First, we estimate four quantities:

- Average for each season in the reference period for the original model.
- Average for each season in the reference period for the downscaled model.
- Average for each season in the future period (2071–2100) for the original model.
- Average for each season in the future period (2071–2100) for the downscaled model.

Then, for each season, we compute the evolution between future and reference periods for the original and downscaled model. We estimate the difference between them and get 4 files in output (one per season). For each season (i.e. for each file), we take the 10th and 90th quantiles of the differences. That gives 4 values for each quantile.

Finally, we control these 4 values are comprised in the following range (unpublished, R. Vautard personal communication):

- temperature between [−2; 2] in K,
- precipitation between [−1; 1] in mm.day-1,
- surface wind speed between [−1; 1] in m.s-1.

In this case, values are higher than previously to account for higher discrepancies but small enough to avoid unrealistic changes. If values are outside the range, the quality control raises an error and the simulation is rejected and thus not included in the dataset.

CRediT Author Statement

T.N.: methodology, software, data curation; **H.L.:** supervision, funding acquisition and writing revue and editing; **D.D.:** writing original draft, visualization, **M.V.:** methodology, writing revue and editing; **G.L.:** resources, software.

Declaration of Competing Interest

The authors declare that they have no known competing financial interests or personal relationships that have or could be perceived to have influenced the work reported in this article.

Acknowledgments

The activities described in this paper were funded by the Copernicus Climate Change Service. ECMWF implements the Copernicus Climate Change Service and the Copernicus Atmosphere Monitoring Service on behalf of the European Commission. To process the data, this study benefited from the IPSL mesocenter ESPRI facility that is supported by CNRS, SU, and Ecole Polytechnique partly funded by IS-ENES3 project. We also thank the Institut Pierre Simon Laplace for assistance with the Synda software and the Deutsches Klimarechenzentrum for the Quality Assurance tool.

Annex 1 – List of data files

Temperature for RCP8.5

tasAdjust_Amon_ACCESS1–0_rcp85_r1i1p1_gr025_TCDF-CDFT23-ERA5–1981–2010_195101–210012.nc
tasAdjust_Amon_ACCESS1–3_rcp85_r1i1p1_gr025_TCDF-CDFT23-ERA5–1981–2010_195101–210012.nc
tasAdjust_Amon_bcc-csm1–1-m_rcp85_r1i1p1_gr025_TCDF-CDFT23-ERA5–1981–2010_195101–210012.nc
tasAdjust_Amon_bcc-csm1–1_rcp85_r1i1p1_gr025_TCDF-CDFT23-ERA5–1981–2010_195101–209912.nc
tasAdjust_Amon_BNU-ESM_rcp85_r1i1p1_gr025_TCDF-CDFT23-ERA5–1981–2010_195101–210012.nc
tasAdjust_Amon_CMCC–CM_rcp85_r1i1p1_gr025_TCDF-CDFT23-ERA5–1981–2010_195101–210012.nc
tasAdjust_Amon_CMCC–CMS_rcp85_r1i1p1_gr025_TCDF-CDFT23-ERA5–1981–2010_195101–210012.nc
tasAdjust_Amon_GFDL-CM3_rcp85_r1i1p1_gr025_TCDF-CDFT23-ERA5–1981–2010_195101–210012.nc
tasAdjust_Amon_GFDL-ESM2G_rcp85_r1i1p1_gr025_TCDF-CDFT23-ERA5–1981–2010_195101–210012.nc
tasAdjust_Amon_GFDL-ESM2M_rcp85_r1i1p1_gr025_TCDF-CDFT23-ERA5–1981–2010_195101–210012.nc
tasAdjust_Amon_HadGEM2-CC_rcp85_r1i1p1_gr025_TCDF-CDFT23-ERA5–1981–2010_195101–210012.nc
tasAdjust_Amon_HadGEM2-ES_rcp85_r1i1p1_gr025_TCDF-CDFT23-ERA5–1981–2010_195101–209908.nc
tasAdjust_Amon_inmcm4_rcp85_r1i1p1_gr025_TCDF-CDFT23-ERA5–1981–2010_195101–210012.nc
tasAdjust_Amon_IPSL-CM5A-LR_rcp85_r1i1p1_gr025_TCDF-CDFT23-ERA5–1981–2010_195101–210012.nc
tasAdjust_Amon_IPSL-CM5A-MR_rcp85_r1i1p1_gr025_TCDF-CDFT23-ERA5–1981–2010_195101–210012.nc
tasAdjust_Amon_IPSL-CM5B-LR_rcp85_r1i1p1_gr025_TCDF-CDFT23-ERA5–1981–2010_195101–210012.nc
tasAdjust_Amon_MIROC5_rcp85_r1i1p1_gr025_TCDF-CDFT23-ERA5–1981–2010_195101–210012.nc
tasAdjust_Amon_MPI-ESM-LR_rcp85_r1i1p1_gr025_TCDF-CDFT23-ERA5–1981–2010_195101–210012.nc
tasAdjust_Amon_MPI-ESM-MR_rcp85_r1i1p1_gr025_TCDF-CDFT23-ERA5–1981–2010_195101–210012.nc
tasAdjust_Amon_NorESM1-M_rcp85_r1i1p1_gr025_TCDF-CDFT23-ERA5–1981–2010_195101–210012.nc

Maximum Temperature for RCP8.5

tasmaxAdjust_Amon_ACCESS1–0_rcp85_r1i1p1_gr025_TCDF-CDFT23-ERA5–1981–2010_195101–210012.nc
tasmaxAdjust_Amon_ACCESS1–3_rcp85_r1i1p1_gr025_TCDF-CDFT23-ERA5–1981–2010_195101–210012.nc
tasmaxAdjust_Amon_bcc-csm1–1-m_rcp85_r1i1p1_gr025_TCDF-CDFT23-ERA5–1981–2010_195101–210012.nc
tasmaxAdjust_Amon_bcc-csm1–1_rcp85_r1i1p1_gr025_TCDF-CDFT23-ERA5–1981–2010_195101–209912.nc
tasmaxAdjust_Amon_BNU-ESM_rcp85_r1i1p1_gr025_TCDF-CDFT23-ERA5–1981–2010_195101–210012.nc
tasmaxAdjust_Amon_CMCC–CM_rcp85_r1i1p1_gr025_TCDF-CDFT23-ERA5–1981–2010_195101–210012.nc
tasmaxAdjust_Amon_CMCC–CMS_rcp85_r1i1p1_gr025_TCDF-CDFT23-ERA5–1981–2010_195101–210012.nc
tasmaxAdjust_Amon_GFDL-CM3_rcp85_r1i1p1_gr025_TCDF-CDFT23-ERA5–1981–2010_195101–210012.nc
tasmaxAdjust_Amon_GFDL-ESM2G_rcp85_r1i1p1_gr025_TCDF-CDFT23-ERA5–1981–2010_195101–210012.nc
tasmaxAdjust_Amon_GFDL-ESM2M_rcp85_r1i1p1_gr025_TCDF-CDFT23-ERA5–1981–2010_195101–210012.nc
tasmaxAdjust_Amon_HadGEM2-CC_rcp85_r1i1p1_gr025_TCDF-CDFT23-ERA5–1981–2010_195101–210012.nc
tasmaxAdjust_Amon_HadGEM2-ES_rcp85_r1i1p1_gr025_TCDF-CDFT23-ERA5–1981–2010_195101–209908.nc
tasmaxAdjust_Amon_inmcm4_rcp85_r1i1p1_gr025_TCDF-CDFT23-ERA5–1981–2010_195101–210012.nc
tasmaxAdjust_Amon_IPSL-CM5A-LR_rcp85_r1i1p1_gr025_TCDF-CDFT23-ERA5–1981–2010_195101–210012.nc
tasmaxAdjust_Amon_IPSL-CM5A-MR_rcp85_r1i1p1_gr025_TCDF-CDFT23-ERA5–1981–2010_195101–210012.nc
tasmaxAdjust_Amon_IPSL-CM5B-LR_rcp85_r1i1p1_gr025_TCDF-CDFT23-ERA5–1981–2010_195101–210012.nc
tasmaxAdjust_Amon_MIROC5_rcp85_r1i1p1_gr025_TCDF-CDFT23-ERA5–1981–2010_195101–210012.nc
tasmaxAdjust_Amon_MPI-ESM-LR_rcp85_r1i1p1_gr025_TCDF-CDFT23-ERA5–1981–2010_195101–210012.nc
tasmaxAdjust_Amon_MPI-ESM-MR_rcp85_r1i1p1_gr025_TCDF-CDFT23-ERA5–1981–2010_195101–210012.nc
tasmaxAdjust_Amon_NorESM1-M_rcp85_r1i1p1_gr025_TCDF-CDFT23-ERA5–1981–2010_195101–210012.nc

Minimum Temperature for RCP8.5

tasminAdjust_Amon_ACCESS1–0_rcp85_r1i1p1_gr025_TCDF-CDFT23-ERA5–1981–2010_195101–210012.nc
tasminAdjust_Amon_ACCESS1–3_rcp85_r1i1p1_gr025_TCDF-CDFT23-ERA5–1981–2010_195101–210012.nc
tasminAdjust_Amon_bcc-csm1–1-m_rcp85_r1i1p1_gr025_TCDF-CDFT23-ERA5–1981–2010_195101–210012.nc
tasminAdjust_Amon_bcc-csm1–1_rcp85_r1i1p1_gr025_TCDF-CDFT23-ERA5–1981–2010_195101–209912.nc
tasminAdjust_Amon_BNU-ESM_rcp85_r1i1p1_gr025_TCDF-CDFT23-ERA5–1981–2010_195101–210012.nc
tasminAdjust_Amon_CMCC–CM_rcp85_r1i1p1_gr025_TCDF-CDFT23-ERA5–1981–2010_195101–210012.nc
tasminAdjust_Amon_CMCC–CMS_rcp85_r1i1p1_gr025_TCDF-CDFT23-ERA5–1981–2010_195101–210012.nc
tasminAdjust_Amon_GFDL-CM3_rcp85_r1i1p1_gr025_TCDF-CDFT23-ERA5–1981–2010_195101–210012.nc
tasminAdjust_Amon_GFDL-ESM2G_rcp85_r1i1p1_gr025_TCDF-CDFT23-ERA5–1981–2010_195101–210012.nc
tasminAdjust_Amon_GFDL-ESM2M_rcp85_r1i1p1_gr025_TCDF-CDFT23-ERA5–1981–2010_195101–210012.nc
tasminAdjust_Amon_HadGEM2-CC_rcp85_r1i1p1_gr025_TCDF-CDFT23-ERA5–1981–2010_195101–210012.nc
tasminAdjust_Amon_HadGEM2-ES_rcp85_r1i1p1_gr025_TCDF-CDFT23-ERA5–1981–2010_195101–209908.nc
tasminAdjust_Amon_inmcm4_rcp85_r1i1p1_gr025_TCDF-CDFT23-ERA5–1981–2010_195101–210012.nc
tasminAdjust_Amon_IPSL-CM5A-LR_rcp85_r1i1p1_gr025_TCDF-CDFT23-ERA5–1981–2010_195101–210012.nc
tasminAdjust_Amon_IPSL-CM5A-MR_rcp85_r1i1p1_gr025_TCDF-CDFT23-ERA5–1981–2010_195101–210012.nc
tasminAdjust_Amon_IPSL-CM5B-LR_rcp85_r1i1p1_gr025_TCDF-CDFT23-ERA5–1981–2010_195101–210012.nc
tasminAdjust_Amon_MIROC5_rcp85_r1i1p1_gr025_TCDF-CDFT23-ERA5–1981–2010_195101–210012.nc
tasminAdjust_Amon_MPI-ESM-LR_rcp85_r1i1p1_gr025_TCDF-CDFT23-ERA5–1981–2010_195101–210012.nc
tasminAdjust_Amon_MPI-ESM-MR_rcp85_r1i1p1_gr025_TCDF-CDFT23-ERA5–1981–2010_195101–210012.nc
tasminAdjust_Amon_NorESM1-M_rcp85_r1i1p1_gr025_TCDF-CDFT23-ERA5–1981–2010_195101–210012.nc

Precipitation for RCP8.5

prAdjust_Amon_ACCESS1–0_rcp85_r1i1p1_gr025_TCDF-CDFT23-ERA5–1981–2010_195101–210012.nc
prAdjust_Amon_ACCESS1–3_rcp85_r1i1p1_gr025_TCDF-CDFT23-ERA5–1981–2010_195101–210012.nc
prAdjust_Amon_bcc-csm1–1-m_rcp85_r1i1p1_gr025_TCDF-CDFT23-ERA5–1981–2010_195101–210012.nc
prAdjust_Amon_BNU-ESM_rcp85_r1i1p1_gr025_TCDF-CDFT23-ERA5–1981–2010_195101–210012.nc
prAdjust_Amon_CMCC–CMS_rcp85_r1i1p1_gr025_TCDF-CDFT23-ERA5–1981–2010_195101–210012.nc
prAdjust_Amon_GFDL-CM3_rcp85_r1i1p1_gr025_TCDF-CDFT23-ERA5–1981–2010_195101–210012.nc
prAdjust_Amon_GFDL-ESM2G_rcp85_r1i1p1_gr025_TCDF-CDFT23-ERA5–1981–2010_195101–210012.nc
prAdjust_Amon_GFDL-ESM2M_rcp85_r1i1p1_gr025_TCDF-CDFT23-ERA5–1981–2010_195101–210012.nc
prAdjust_Amon_HadGEM2-CC_rcp85_r1i1p1_gr025_TCDF-CDFT23-ERA5–1981–2010_195101–210012.nc
prAdjust_Amon_HadGEM2-ES_rcp85_r1i1p1_gr025_TCDF-CDFT23-ERA5–1981–2010_195101–209908.nc
prAdjust_Amon_inmcm4_rcp85_r1i1p1_gr025_TCDF-CDFT23-ERA5–1981–2010_195101–210012.nc
prAdjust_Amon_IPSL-CM5A-LR_rcp85_r1i1p1_gr025_TCDF-CDFT23-ERA5–1981–2010_195101–210012.nc
prAdjust_Amon_IPSL-CM5A-MR_rcp85_r1i1p1_gr025_TCDF-CDFT23-ERA5–1981–2010_195101–210012.nc
prAdjust_Amon_IPSL-CM5B-LR_rcp85_r1i1p1_gr025_TCDF-CDFT23-ERA5–1981–2010_195101–210012.nc
prAdjust_Amon_MIROC5_rcp85_r1i1p1_gr025_TCDF-CDFT23-ERA5–1981–2010_195101–210012.nc
prAdjust_Amon_MPI-ESM-LR_rcp85_r1i1p1_gr025_TCDF-CDFT23-ERA5–1981–2010_195101–210012.nc
prAdjust_Amon_MPI-ESM-MR_rcp85_r1i1p1_gr025_TCDF-CDFT23-ERA5–1981–2010_195101–210012.nc
prAdjust_Amon_NorESM1-M_rcp85_r1i1p1_gr025_TCDF-CDFT23-ERA5–1981–2010_195101–210012.nc

Wind speed for RCP8.5

sfcWindAdjust_Amon_ACCESS1–0_rcp85_r1i1p1_gr025_TCDF-CDFT23-ERA5–1981–2010_195101–210012.nc
sfcWindAdjust_Amon_ACCESS1–3_rcp85_r1i1p1_gr025_TCDF-CDFT23-ERA5–1981–2010_195101–210012.nc
sfcWindAdjust_Amon_BNU-ESM_rcp85_r1i1p1_gr025_TCDF-CDFT23-ERA5–1981–2010_195101–210012.nc
sfcWindAdjust_Amon_CMCC–CMS_rcp85_r1i1p1_gr025_TCDF-CDFT23-ERA5–1981–2010_195101–210012.nc
sfcWindAdjust_Amon_GFDL-CM3_rcp85_r1i1p1_gr025_TCDF-CDFT23-ERA5–1981–2010_195101–210012.nc
sfcWindAdjust_Amon_GFDL-ESM2G_rcp85_r1i1p1_gr025_TCDF-CDFT23-ERA5–1981–2010_195101–210012.nc
sfcWindAdjust_Amon_GFDL-ESM2M_rcp85_r1i1p1_gr025_TCDF-CDFT23-ERA5–1981–2010_195101–210012.nc
sfcWindAdjust_Amon_HadGEM2-CC_rcp85_r1i1p1_gr025_TCDF-CDFT23-ERA5–1981–2010_195101–210012.nc
sfcWindAdjust_Amon_HadGEM2-ES_rcp85_r1i1p1_gr025_TCDF-CDFT23-ERA5–1981–2010_195101–209908.nc
sfcWindAdjust_Amon_IPSL-CM5A-LR_rcp85_r1i1p1_gr025_TCDF-CDFT23-ERA5–1981–2010_195101–210012.nc
sfcWindAdjust_Amon_IPSL-CM5A-MR_rcp85_r1i1p1_gr025_TCDF-CDFT23-ERA5–1981–2010_195101–210012.nc
sfcWindAdjust_Amon_IPSL-CM5B-LR_rcp85_r1i1p1_gr025_TCDF-CDFT23-ERA5–1981–2010_195101–210012.nc
sfcWindAdjust_Amon_MIROC5_rcp85_r1i1p1_gr025_TCDF-CDFT23-ERA5–1981–2010_195101–210012.nc
sfcWindAdjust_Amon_MPI-ESM-LR_rcp85_r1i1p1_gr025_TCDF-CDFT23-ERA5–1981–2010_195101–210012.nc
sfcWindAdjust_Amon_MPI-ESM-MR_rcp85_r1i1p1_gr025_TCDF-CDFT23-ERA5–1981–2010_195101–210012.nc

Temperature for RCP4.5

tasAdjust_Amon_ACCESS1–0_rcp45_r1i1p1_gr025_TCDF-CDFT23-ERA5–1981–2010_195101–210012.nc
tasAdjust_Amon_ACCESS1–3_rcp45_r1i1p1_gr025_TCDF-CDFT23-ERA5–1981–2010_195101–210012.nc
tasAdjust_Amon_bcc-csm1–1-m_rcp45_r1i1p1_gr025_TCDF-CDFT23-ERA5–1981–2010_195101–210012.nc
tasAdjust_Amon_bcc-csm1–1_rcp45_r1i1p1_gr025_TCDF-CDFT23-ERA5–1981–2010_195101–210012.nc
tasAdjust_Amon_BNU-ESM_rcp45_r1i1p1_gr025_TCDF-CDFT23-ERA5–1981–2010_195101–210012.nc
tasAdjust_Amon_CMCC–CM_rcp45_r1i1p1_gr025_TCDF-CDFT23-ERA5–1981–2010_195101–210012.nc
tasAdjust_Amon_CNRM-CM5_rcp45_r1i1p1_gr025_TCDF-CDFT23-ERA5–1981–2010_195101–210012.nc
tasAdjust_Amon_GFDL-CM3_rcp45_r1i1p1_gr025_TCDF-CDFT23-ERA5–1981–2010_195101–210012.nc
tasAdjust_Amon_GFDL-ESM2G_rcp45_r1i1p1_gr025_TCDF-CDFT23-ERA5–1981–2010_195101–210012.nc
tasAdjust_Amon_GFDL-ESM2M_rcp45_r1i1p1_gr025_TCDF-CDFT23-ERA5–1981–2010_195101–210012.nc
tasAdjust_Amon_HadGEM2-CC_rcp45_r1i1p1_gr025_TCDF-CDFT23-ERA5–1981–2010_195101–210012.nc
tasAdjust_Amon_HadGEM2-ES_rcp45_r1i1p1_gr025_TCDF-CDFT23-ERA5–1981–2010_195101–209908.nc
tasAdjust_Amon_inmcm4_rcp45_r1i1p1_gr025_TCDF-CDFT23-ERA5–1981–2010_195101–210012.nc
tasAdjust_Amon_IPSL-CM5A-LR_rcp45_r1i1p1_gr025_TCDF-CDFT23-ERA5–1981–2010_195101–210012.nc
tasAdjust_Amon_IPSL-CM5A-MR_rcp45_r1i1p1_gr025_TCDF-CDFT23-ERA5–1981–2010_195101–210012.nc
tasAdjust_Amon_IPSL-CM5B-LR_rcp45_r1i1p1_gr025_TCDF-CDFT23-ERA5–1981–2010_195101–210012.nc
tasAdjust_Amon_MIROC5_rcp45_r1i1p1_gr025_TCDF-CDFT23-ERA5–1981–2010_195101–210012.nc
tasAdjust_Amon_MPI-ESM-LR_rcp45_r1i1p1_gr025_TCDF-CDFT23-ERA5–1981–2010_195101–210012.nc
tasAdjust_Amon_MPI-ESM-MR_rcp45_r1i1p1_gr025_TCDF-CDFT23-ERA5–1981–2010_195101–210012.nc
tasAdjust_Amon_NorESM1-M_rcp45_r1i1p1_gr025_TCDF-CDFT23-ERA5–1981–2010_195101–210012.nc

Maximum Temperature for RCP4.5

tasmaxAdjust_Amon_ACCESS1–0_rcp45_r1i1p1_gr025_TCDF-CDFT23-ERA5–1981–2010_195101–210012.nc
tasmaxAdjust_Amon_ACCESS1–3_rcp45_r1i1p1_gr025_TCDF-CDFT23-ERA5–1981–2010_195101–210012.nc
tasmaxAdjust_Amon_bcc-csm1–1-m_rcp45_r1i1p1_gr025_TCDF-CDFT23-ERA5–1981–2010_195101–210012.nc
tasmaxAdjust_Amon_bcc-csm1–1_rcp45_r1i1p1_gr025_TCDF-CDFT23-ERA5–1981–2010_195101–210012.nc
tasmaxAdjust_Amon_BNU-ESM_rcp45_r1i1p1_gr025_TCDF-CDFT23-ERA5–1981–2010_195101–210012.nc
tasmaxAdjust_Amon_CMCC–CM_rcp45_r1i1p1_gr025_TCDF-CDFT23-ERA5–1981–2010_195101–210012.nc
tasmaxAdjust_Amon_CNRM-CM5_rcp45_r1i1p1_gr025_TCDF-CDFT23-ERA5–1981–2010_195101–210012.nc
tasmaxAdjust_Amon_GFDL-CM3_rcp45_r1i1p1_gr025_TCDF-CDFT23-ERA5–1981–2010_195101–210012.nc
tasmaxAdjust_Amon_GFDL-ESM2G_rcp45_r1i1p1_gr025_TCDF-CDFT23-ERA5–1981–2010_195101–210012.nc
tasmaxAdjust_Amon_GFDL-ESM2M_rcp45_r1i1p1_gr025_TCDF-CDFT23-ERA5–1981–2010_195101–210012.nc
tasmaxAdjust_Amon_HadGEM2-CC_rcp45_r1i1p1_gr025_TCDF-CDFT23-ERA5–1981–2010_195101–210012.nc
tasmaxAdjust_Amon_HadGEM2-ES_rcp45_r1i1p1_gr025_TCDF-CDFT23-ERA5–1981–2010_195101–209908.nc
tasmaxAdjust_Amon_inmcm4_rcp45_r1i1p1_gr025_TCDF-CDFT23-ERA5–1981–2010_195101–210012.nc
tasmaxAdjust_Amon_IPSL-CM5A-LR_rcp45_r1i1p1_gr025_TCDF-CDFT23-ERA5–1981–2010_195101–210012.nc
tasmaxAdjust_Amon_IPSL-CM5A-MR_rcp45_r1i1p1_gr025_TCDF-CDFT23-ERA5–1981–2010_195101–210012.nc
tasmaxAdjust_Amon_IPSL-CM5B-LR_rcp45_r1i1p1_gr025_TCDF-CDFT23-ERA5–1981–2010_195101–210012.nc
tasmaxAdjust_Amon_MIROC5_rcp45_r1i1p1_gr025_TCDF-CDFT23-ERA5–1981–2010_195101–210012.nc
tasmaxAdjust_Amon_MPI-ESM-LR_rcp45_r1i1p1_gr025_TCDF-CDFT23-ERA5–1981–2010_195101–210012.nc
tasmaxAdjust_Amon_MPI-ESM-MR_rcp45_r1i1p1_gr025_TCDF-CDFT23-ERA5–1981–2010_195101–210012.nc
tasmaxAdjust_Amon_NorESM1-M_rcp45_r1i1p1_gr025_TCDF-CDFT23-ERA5–1981–2010_195101–210012.nc

Minimum Temperature for RCP4.5

tasminAdjust_Amon_ACCESS1–0_rcp45_r1i1p1_gr025_TCDF-CDFT23-ERA5–1981–2010_195101–210012.nc
tasminAdjust_Amon_ACCESS1–3_rcp45_r1i1p1_gr025_TCDF-CDFT23-ERA5–1981–2010_195101–210012.nc
tasminAdjust_Amon_bcc-csm1–1-m_rcp45_r1i1p1_gr025_TCDF-CDFT23-ERA5–1981–2010_195101–210011.nc
tasminAdjust_Amon_bcc-csm1–1_rcp45_r1i1p1_gr025_TCDF-CDFT23-ERA5–1981–2010_195101–210012.nc
tasminAdjust_Amon_BNU-ESM_rcp45_r1i1p1_gr025_TCDF-CDFT23-ERA5–1981–2010_195101–210012.nc
tasminAdjust_Amon_CMCC–CM_rcp45_r1i1p1_gr025_TCDF-CDFT23-ERA5–1981–2010_195101–210012.nc
tasminAdjust_Amon_CNRM-CM5_rcp45_r1i1p1_gr025_TCDF-CDFT23-ERA5–1981–2010_195101–210012.nc
tasminAdjust_Amon_GFDL-CM3_rcp45_r1i1p1_gr025_TCDF-CDFT23-ERA5–1981–2010_195101–210012.nc
tasminAdjust_Amon_GFDL-ESM2G_rcp45_r1i1p1_gr025_TCDF-CDFT23-ERA5–1981–2010_195101–210012.nc
tasminAdjust_Amon_GFDL-ESM2M_rcp45_r1i1p1_gr025_TCDF-CDFT23-ERA5–1981–2010_195101–210012.nc
tasminAdjust_Amon_HadGEM2-CC_rcp45_r1i1p1_gr025_TCDF-CDFT23-ERA5–1981–2010_195101–210012.nc
tasminAdjust_Amon_HadGEM2-ES_rcp45_r1i1p1_gr025_TCDF-CDFT23-ERA5–1981–2010_195101–209908.nc

tasminAdjust_Amon_inmcm4_rcp45_r1i1p1_gr025_TCDF-CDFT23-ERA5–1981–2010_195101–210012.nc
tasminAdjust_Amon_IPSL-CM5A-LR_rcp45_r1i1p1_gr025_TCDF-CDFT23-ERA5–1981–2010_195101–210012.nc
tasminAdjust_Amon_IPSL-CM5A-MR_rcp45_r1i1p1_gr025_TCDF-CDFT23-ERA5–1981–2010_195101–210012.nc
tasminAdjust_Amon_IPSL-CM5B-LR_rcp45_r1i1p1_gr025_TCDF-CDFT23-ERA5–1981–2010_195101–210012.nc
tasminAdjust_Amon_MIROC5_rcp45_r1i1p1_gr025_TCDF-CDFT23-ERA5–1981–2010_195101–210012.nc
tasminAdjust_Amon_MPI-ESM-LR_rcp45_r1i1p1_gr025_TCDF-CDFT23-ERA5–1981–2010_195101–210012.nc
tasminAdjust_Amon_MPI-ESM-MR_rcp45_r1i1p1_gr025_TCDF-CDFT23-ERA5–1981–2010_195101–210012.nc
tasminAdjust_Amon_NorESM1-M_rcp45_r1i1p1_gr025_TCDF-CDFT23-ERA5–1981–2010_195101–210012.nc

Precipitation for RCP4.5

prAdjust_Amon_ACCESS1–0_rcp45_r1i1p1_gr025_TCDF-CDFT23-ERA5–1981–2010_195101–210012.nc
prAdjust_Amon_ACCESS1–3_rcp45_r1i1p1_gr025_TCDF-CDFT23-ERA5–1981–2010_195101–210012.nc
prAdjust_Amon_bcc-csm1–1-m_rcp45_r1i1p1_gr025_TCDF-CDFT23-ERA5–1981–2010_195101–210010.nc
prAdjust_Amon_bcc-csm1–1_rcp45_r1i1p1_gr025_TCDF-CDFT23-ERA5–1981–2010_195101–210012.nc
prAdjust_Amon_BNU-ESM_rcp45_r1i1p1_gr025_TCDF-CDFT23-ERA5–1981–2010_195101–210012.nc
prAdjust_Amon_CMCC–CM_rcp45_r1i1p1_gr025_TCDF-CDFT23-ERA5–1981–2010_195101–210012.nc
prAdjust_Amon_CNRM-CM5_rcp45_r1i1p1_gr025_TCDF-CDFT23-ERA5–1981–2010_195101–210012.nc
prAdjust_Amon_GFDL-CM3_rcp45_r1i1p1_gr025_TCDF-CDFT23-ERA5–1981–2010_195101–210012.nc
prAdjust_Amon_GFDL-ESM2G_rcp45_r1i1p1_gr025_TCDF-CDFT23-ERA5–1981–2010_195101–210012.nc
prAdjust_Amon_GFDL-ESM2M_rcp45_r1i1p1_gr025_TCDF-CDFT23-ERA5–1981–2010_195101–210012.nc
prAdjust_Amon_HadGEM2-CC_rcp45_r1i1p1_gr025_TCDF-CDFT23-ERA5–1981–2010_195101–210012.nc
prAdjust_Amon_HadGEM2-ES_rcp45_r1i1p1_gr025_TCDF-CDFT23-ERA5–1981–2010_195101–209908.nc
prAdjust_Amon_inmcm4_rcp45_r1i1p1_gr025_TCDF-CDFT23-ERA5–1981–2010_195101–210012.nc
prAdjust_Amon_IPSL-CM5A-LR_rcp45_r1i1p1_gr025_TCDF-CDFT23-ERA5–1981–2010_195101–210012.nc
prAdjust_Amon_IPSL-CM5A-MR_rcp45_r1i1p1_gr025_TCDF-CDFT23-ERA5–1981–2010_195101–210012.nc
prAdjust_Amon_IPSL-CM5B-LR_rcp45_r1i1p1_gr025_TCDF-CDFT23-ERA5–1981–2010_195101–210012.nc
prAdjust_Amon_MIROC5_rcp45_r1i1p1_gr025_TCDF-CDFT23-ERA5–1981–2010_195101–210012.nc
prAdjust_Amon_MPI-ESM-LR_rcp45_r1i1p1_gr025_TCDF-CDFT23-ERA5–1981–2010_195101–210012.nc
prAdjust_Amon_MPI-ESM-MR_rcp45_r1i1p1_gr025_TCDF-CDFT23-ERA5–1981–2010_195101–210012.nc
prAdjust_Amon_NorESM1-M_rcp45_r1i1p1_gr025_TCDF-CDFT23-ERA5–1981–2010_195101–210012.nc

Wind speed for RCP4.5

sfcWindAdjust_Amon_ACCESS1–0_rcp45_r1i1p1_gr025_TCDF-CDFT23-ERA5–1981–2010_195101–210012.nc
sfcWindAdjust_Amon_ACCESS1–3_rcp45_r1i1p1_gr025_TCDF-CDFT23-ERA5–1981–2010_195101–210012.nc
sfcWindAdjust_Amon_BNU-ESM_rcp45_r1i1p1_gr025_TCDF-CDFT23-ERA5–1981–2010_195101–210012.nc
sfcWindAdjust_Amon_CNRM-CM5_rcp45_r1i1p1_gr025_TCDF-CDFT23-ERA5–1981–2010_195101–210012.nc
sfcWindAdjust_Amon_GFDL-CM3_rcp45_r1i1p1_gr025_TCDF-CDFT23-ERA5–1981–2010_195101–210012.nc
sfcWindAdjust_Amon_GFDL-ESM2G_rcp45_r1i1p1_gr025_TCDF-CDFT23-ERA5–1981–2010_195101–210012.nc
sfcWindAdjust_Amon_GFDL-ESM2M_rcp45_r1i1p1_gr025_TCDF-CDFT23-ERA5–1981–2010_195101–210012.nc
sfcWindAdjust_Amon_HadGEM2-CC_rcp45_r1i1p1_gr025_TCDF-CDFT23-ERA5–1981–2010_195101–210012.nc
sfcWindAdjust_Amon_HadGEM2-ES_rcp45_r1i1p1_gr025_TCDF-CDFT23-ERA5–1981–2010_195101–209908.nc
sfcWindAdjust_Amon_IPSL-CM5A-LR_rcp45_r1i1p1_gr025_TCDF-CDFT23-ERA5–1981–2010_195101–210012.nc
sfcWindAdjust_Amon_IPSL-CM5A-MR_rcp45_r1i1p1_gr025_TCDF-CDFT23-ERA5–1981–2010_195101–210012.nc
sfcWindAdjust_Amon_IPSL-CM5B-LR_rcp45_r1i1p1_gr025_TCDF-CDFT23-ERA5–1981–2010_195101–210012.nc
sfcWindAdjust_Amon_MIROC5_rcp45_r1i1p1_gr025_TCDF-CDFT23-ERA5–1981–2010_195101–210012.nc
sfcWindAdjust_Amon_MPI-ESM-LR_rcp45_r1i1p1_gr025_TCDF-CDFT23-ERA5–1981–2010_195101–210012.nc
sfcWindAdjust_Amon_MPI-ESM-MR_rcp45_r1i1p1_gr025_TCDF-CDFT23-ERA5–1981–2010_195101–210012.nc

References

[1] K.E. Taylor, R.J. Stouffer, G.A. Meehl, An overview of CMIP5 and the experiment design, Bull. Am. Meteorol. Soc. 93 (2012) 485–498, doi:10.1175/BAMS-Dd-11-00094.1.

[2] H. Hersbach, B. Bell, P. Berrisford, S. Hirahara, A. Horányi, J. Muñoz-Sabater, J. Nicolas, C. Peubey, R. Radu, D. Schepers, A. Simmons, C. Soci, S. Abdalla, X. Abellan, G. Balsamo, P. Bechtold, G. Biavati, J. Bidlot, M. Bonavita, G. De Chiara, P. Dahlgren, D. Dee, M. Diamantakis, R. Dragani, J. Flemming, R. Forbes, M. Fuentes, A. Geer, L. Haimberger, S. Healy, R.J. Hogan, E. Hólm, M. Janisková, S. Keeley, P. Laloyaux, P. Lopez, C. Lupu, G. Radnoti, P. de Rosnay, I. Rozum, F. Vamborg, S. Villaume, J.N. Thépaut, The ERA5 global reanalysis, Q. J. R. Meteorol. Soc. 146 (2020) 1999–2049, doi:10.1002/qj.3803.

[3] S. Galmarini, A.J. Cannon, A. Ceglar, O.B. Christensen, N. de Noblet-Ducoudré, F. Dentener, F.J. Doblas-Reyes, A. Dosio, J.M. Gutierrez, M. Iturbide, M. Jury, S. Lange, H. Loukos, A. Maiorano, D. Maraun, S. McGinnis, G. Nikulin, A. Riccio, E. Sanchez, E. Solazzo, A. Toreti, M. Vrac, M. Zampieri, Adjusting climate model bias for agricultural impact assessment: how to cut the mustard, Clim. Serv. 13 (2019) 65–69, doi:10.1016/j.cliser.2019.01.004.
[4] G. Levavasseur, T. Noël, Data Reference Syntax (DRS) for bias-adjusted C3S-CMIP5 simulations (2021), doi:10.31223/X5389H.
[5] J.-.L. Dufresne, M. -a. Foujols, S. Denvil, A. Caubel, O. Marti, O. Aumont, Y. Balkanski, S. Bekki, H. Bellenger, R. Benshila, S. Bony, L. Bopp, P. Braconnot, P. Brockmann, P. Cadule, F. Cheruy, F. Codron, A. Cozic, D. Cugnet, N. de Noblet, J.-.P. Duvel, C. Ethé, L. Fairhead, T. Fichefet, S. Flavoni, P. Friedlingstein, J.-.Y. Grandpeix, L. Guez, E. Guilyardi, D. Hauglustaine, F. Hourdin, A. Idelkadi, J. Ghattas, S. Joussaume, M. Kageyama, G. Krinner, S. Labetoulle, A. Lahellec, M.-.P. Lefebvre, F. Lefevre, C. Levy, Z.X. Li, J. Lloyd, F. Lott, G. Madec, M. Mancip, M. Marchand, S. Masson, Y. Meurdesoif, J. Mignot, I. Musat, S. Parouty, J. Polcher, C. Rio, M. Schulz, D. Swingedouw, S. Szopa, C. Talandier, P. Terray, N. Viovy, N. Vuichard, Climate change projections using the IPSL-CM5 Earth System Model: from CMIP3 to CMIP5, Clim. Dyn. 40 (2013) 2123–2165, doi:10.1007/s00382-012-1636-1.
[6] P. Michelangeli, M. Vrac, H. Loukos, Probabilistic downscaling approaches: application to wind cumulative distribution functions, Geophys. Res. Lett. 36 (2009) L11708, doi:10.1029/2009GL038401.
[7] M. Vrac, P. Drobinski, A. Merlo, M. Herrmann, C. Lavaysse, L. Li, S. Somot, Dynamical and statistical downscaling of the French Mediterranean climate: uncertainty assessment, Nat. Hazards Earth Syst. Sci. 12 (2012) 2769–2784, doi:10.5194/nhess-12-2769-2012.
[8] R. Vautard, T. Noël, L. Li, M. Vrac, E. Martin, P. Dandin, J. Cattiaux, S. Joussaume, Climate variability and trends in downscaled high-resolution simulations and projections over Metropolitan France, Clim. Dyn. 41 (2013) 1419–1437, doi:10.1007/s00382-012-1621-8.
[9] A.M. Famien, S. Janicot, A.D. Ochou, M. Vrac, D. Defrance, B. Sultan, T. Noël, A bias-corrected CMIP5 dataset for Africa using the CDF-t method – a contribution to agricultural impact studies, Earth Syst. Dyn. 9 (2018) 313–338, doi:10.5194/esd-9-313-2018.
[10] B. Bartók, I. Tobin, R. Vautard, M. Vrac, X. Jin, G. Levavasseur, S. Denvil, L. Dubus, S. Parey, P.A. Michelangeli, A. Troccoli, Y.M. Saint-Drenan, A climate projection dataset tailored for the European energy sector, Clim. Serv. 16 (2019) 100138, doi:10.1016/j.cliser.2019.100138.
[11] D. Defrance, G. Ramstein, S. Charbit, M. Vrac, A.M. Famien, B. Sultan, D. Swingedouw, C. Dumas, F. Gemenne, J. Alvarez-Solas, Consequences of rapid ice sheet melting on the Sahelian population vulnerability, Proc. Natl. Acad. Sci. 114 (2017) 6533–6538, doi:10.1073/pnas.1619358114.
[12] D. Defrance, B. Sultan, M. Castets, A.M. Famien, C. Baron, Impact of climate change in West Africa on cereal production per capita in 2050, Sustain 12 (2020) 1–19, doi:10.3390/su12187585.
[13] B. Rhoné, D. Defrance, C. Berthouly-Salazar, C. Mariac, P. Cubry, M. Couderc, A. Dequincey, A. Assoumanne, N.A. Kane, B. Sultan, A. Barnaud, Y. Vigouroux, Pearl millet genomic vulnerability to climate change in West Africa highlights the need for regional collaboration, Nat. Commun. 11 (2020), doi:10.1038/s41467-020-19066-4.
[14] D. Maraun, Bias correcting climate change simulations - a critical review, Curr. Clim. Chang. Rep. 2 (2016) 211–220, doi:10.1007/s40641-016-0050-x.
[15] M. Vrac, T. Noël, R. Vautard, Bias correction of precipitation through singularity stochastic removal: because occurrences matter, J. Geophys. Res. 121 (2016) 5237–5258, doi:10.1002/2015JD024511.